PulmoBind, an Adrenomedullin-Based Molecular Lung Imaging Tool

Short Running Foot Line: PulmoBind Lung Imaging

Myriam Létourneau[§1], Quang Trinh Nguyen[§2], François Harel[2,3], Alain Fournier[1] and Jocelyn Dupuis[2,4]

[1]INRS-Institut Armand-Frappier, Laboratoire d'études moléculaires et pharmacologiques des peptides, Laval, QC, Canada;

[2]Research Centre, Montreal Heart Institute, Montreal, QC, Canada;

Departments of [3]Radiology and [4]Medicine, Université de Montréal, Montreal, QC, Canada

Corresponding author: Jocelyn Dupuis, MD, PhD, Research Center, Montreal Heart Institute, 5000 Belanger Street, Montreal, QC, Canada, H1T 1C8.

Tel.: (514) 376-3330 ext. 3542; Fax: (514) 376-1355

E-mail: jocelyn.dupuis@bellnet.ca

[§]Authors have contributed equally to this work.

First Authors:

Myriam Létourneau, M.Sc., INRS-Institut Armand-Frappier, 531 boul. des Prairies, Laval, QC, Canada, H7V 1B7; Tel.: (450) 687-5010 ext.8803; Fax: (450) 686-5566

E-mail: myriam.letourneau@iaf.inrs.ca

Quang Trinh Nguyen, Ph.D, Montreal Heart Institute, 5000 Belanger Street, Montreal, QC, Canada, H1T 1C8; Tel.: (514)376-3330 ext.3479; Fax: (514)376-1355

E-mail: quangtrinhn@yahoo.com

Word Count: 6381

Financial Support: This work was supported by PulmoScience Inc., Canadian Institutes of Health Research, and Montreal Heart Institute Foundation.

Conflict of Interest: Dr. Jocelyn Dupuis is scientific director and a shareholder of PulmoScience.

Abstract

Previous studies showed that adrenomedullin (AM) could be a promising molecular imaging agent for the pulmonary circulation with abundant specific binding sites at the pulmonary vascular endothelium. The purpose of this work was to design an AM-based compound that encompasses the desired imaging properties without arising safety issues for clinical applications.

Methods: AM analogs were synthesized through solid phase peptide synthesis. They were evaluated for ^{99m}Tc labeling efficiency and *in vivo* lung uptake. Biodistribution and hemodynamic characteristics of the lead compound were determined in anesthetized dogs as well as a dosimetric analysis. Lung perfusion was evaluated in the monocrotaline model of pulmonary arterial hypertension (PAH) in rats.

Results: A cyclic AM(22-52) analog encompassing a polyethylene glycol spacer and a tetrapeptide chelating moiety was found to possess the desired characteristics with 90.7% ± 0.3% labeling efficiency, 40% lung uptake at 10min post-injection and a favorable safety profile. Lung uptake of the ^{99m}Tc-labeled compound was importantly reduced in PAH.

Conclusion: This lead compound, named PulmoBind, could be a suitable clinical imaging agent for the molecular diagnosis of disorders of the pulmonary circulation.

Key Words: lung; molecular imaging; adrenomedullin; nuclear medicine; pulmonary hypertension

Introduction

On one hand, pulmonary embolism (PE) is a potentially lethal lung perfusion defect that commonly develops in patients suffering from deep vein thrombosis (*1*). On the other hand, pulmonary hypertension (PH), a disorder with various etiologies, leads in its most severe forms to right ventricular failure and death (*2*). Diagnosis of these pathologies is challenging because patients often present with a non-specific symptom, shortness of breath. Currently, nuclear imaging of the pulmonary circulation can be achieved through the use of ^{99m}Tc-albumin macro-aggregates, particles that are trapped in the microvasculature due to their size (10-150 µm) in proportion to the regional blood flow (*3*). However, this technique lacks the ability to detect functional perfusion defects while uncovering of small blood vessel blockade is limited. Moreover, this tracer blocks pulmonary blood vessels in subjects with an already compromised pulmonary circulation while increasing the potential infectious risk because it is prepared from human albumin. We have recently shown that adrenomedullin (AM) is a very promising molecular lung imaging tool for the diagnosis of pathologies such as PE and PH (*4,5*). AM, a peptide from the calcitonin family, allows specific lung imaging through binding with its specific receptor AM1 (CRLR/Ramp2), expressed in high density in pulmonary vessels (*6,7*). Enhanced imaging efficiency can be associated with cell internalization after receptor activation by its agonist (*8,9*) but this process is also correlated with inherent biological activity.

Conversely, antagonists do not evoke cellular activation upon receptor binding while being able to bind with uniform affinity to the total pool of receptors (*10,11*).

AM is a 52-amino acid multifunctional regulatory peptide widely distributed and acting mainly in the cardiovascular system where it is classically described as a vasodilator (*12*). Previous structure-activity relationship studies have demonstrated that truncation of the N-terminal stretch while keeping the cyclic structure formed by a disulfide bridge between residues 16 and 21 generated agonists, such as AM(13-52) and AM(16-52), with similar affinity to the full length peptide (*13*). Further truncation at the N-terminus to remove the ring structure yields the only fully characterized human AM antagonist, i.e. AM(22-52) while removal of the C-terminal amino acid greatly diminishes binding affinity and peptide activity (*13,14*). Interestingly, analogs composed only of the ring structure, i.e. AM(15-22) and AM(16-21), increase systemic arterial blood pressure (*15*) but AM(1-25) and AM(1-40) were unable to displace ^{125}I-AM in a dog lung homogenate binding experiment (*6*). Moreover, linearization of the full-length peptide resulted in a loss of affinity (*6,13*). Finally, although AM is quite a long peptide, incorporation of a radionuclide can affect its binding ability and therefore AM-derived nuclear imaging tools should favour radiolabeling at the N-terminus of the peptide (*16*).

AM(22-52) is an antagonist having 10 times less affinity for its receptors than AM(13-52) in competition displacement experiments, but with higher selectivity for

AM1 over AM2 (CRLR/Ramp3) (*6,14*). Thus, this peptide appeared has a good starting point to generate new AM antagonists suitable for nuclear lung imaging. Such an analog would enable pulmonary microcirculation imaging without any side effects on blood pressure. Furthermore and as pointed out for AM, such a molecule would not only be valuable to detect perfusion defects but could also allow the detection of early endothelium related deficiencies such as PH.

In this article, we describe the design, synthesis and characterization of PulmoBind, an AM-based analog for pulmonary circulation imaging. This new molecular lung imaging tool shows good binding affinity, high ^{99m}Tc labeling efficiency, significant lung uptake even after 1h without any effect on mean arterial pressure (MAP).

This molecule could offer the possibility not only to detect large pulmonary vessel blockade such as PE, but also allow detection of anatomical and, potentially, functional pulmonary microcirculatory disorders caused by the various forms of PH. Thus, PulmoBind could provide an efficient, safe and non-invasive method to probe the status of the pulmonary circulation.

MATERIALS AND METHODS

All animal experimental procedures were performed in accordance with regulations and ethical guidelines from the Canadian Council for the Care of Laboratory Animals, and received approval by the animal ethics and research committee of the Montreal Heart Institute.

AM Derivative Synthesis and Purification

AM-derived peptides were synthesized and purified as described previously (*6*). The N-Fmoc-amino-d-Polyethylene glycol $(PEG)_4$-acid used as a spacer in the peptide synthesis was purchased from Quanta Biodesign Ltd. (Powell, OH, USA). Disulfide bond formation to give cyclic derivatives was performed with an overnight air oxidation after dissolution of the linear peptide in an aqueous solution (pH 8.8) at a concentration of 0.1 mg/mL. Peptides were purified by reversed phase-HPLC. Amino acid sequences of synthesized peptides are given in Table 1 along with purity of final products and molecular mass as evaluated by Maldi-Tof mass spectrometry (Voyager DE, Applied Biosystems, CA, USA).

^{99m}Tc-Labeling

Linear AM was radiolabeled through its cysteine residues as previously described (*5*). For AM analogs containing a chelator moiety, 2.29 nmol of lyophilized peptide were resuspended in 20 µL of acetate buffer 1 M (pH 5.5) to which 200 µL of

Na_3PO_4 0.1 M (pH 12) and 31.25 µL of freshly prepared $SnCl_2$ solution (0.8 mg/mL, in HCl 0.05 M) were added. Immediately after dissolution, sterile and fresh daily prepared $Na^{99m}TcO_4$ (185-555 MBq) in a sodium chloride injection USP solution was added to the mixture. The mixture was kept at room temperature for 15 min and 1 mL of NaH_2PO_4 0.1M (pH 4.5) was finally added. Radiochemical purity and labeling efficiency was assessed through instant thin layer chromatography on silica gel impregnated glass fiber paper (ITLC-SG) using acetone for dosage of free ^{99m}Tc and BAP (37.5% (v/v) butanol, 7.5% (v/v) acetic acid and 30% (v/v) pyridine in water) to discriminate ^{99m}Tc-colloids (bottom) from radiolabeled peptide (top).

To purify ^{99m}Tc-AM derivatives, the radiolabeling reaction mixture was injected onto a 1-mL (100-mg) C_{18} Sep-Pak (Waters) cartridge. The cartridge was then washed with 3 mL of hydrochloric acid (1 mM) and eluted with 3 mL of a 50% (v/v) ethanol/ water solution. Fractions of 0.5 mL were collected into sterile polypropylene tubes. Fractions with the highest counts were pooled and 200 µL of 10X concentrated PBS (pH 7.4) were added for stabilization.

In vivo Biodistribution and Lung Uptake

Mongrel dogs (20-30kg) were anesthetized by intravenous injection of sodium pentobarbital (50 mg/kg), intubated and mechanically ventilated. Purified ^{99m}Tc-AM derivatives (185 MBq) were injected intravenously (i.v.) *via* the jugular vein through a three-way stopcock 18-French catheter for lung uptake evaluation. *In vivo* whole body biodistribution of radiolabeled peptide was evaluated with a dual-head gamma

camera (Siemens, Burlington, ON, Canada) equipped with a low-energy parallel-hole collimator. Dynamic acquisitions were recorded for a 30 min period and static whole body scans were performed at 30, 60 and 120 min after ^{99m}Tc-labeled peptide injection at a scan speed of 10 cm/min. Dynamic and static acquisitions were evaluated using MATLAB version 7.01 image analysis tools software. Data correction was applied for radioactive decay, table adjustment (dorsal images only), geometric mean, and organ's attenuation based on transmission factor. Results were expressed as a percentage of the total radioactivity injected.

Binding Assays

The binding ability of PulmoBind was evaluated in dog lung homogenates prepared as previously described (*6*). Briefly, lungs were diced, homogenized and centrifuged at 49000 g at 4°C for 20min. Pellets were washed twice and non-homogenized tissue was removed by gentle centrifugation (500 g, 5 min). Aliquots of the supernatant were kept at -80°C until used for binding assays. Binding experiments were based on protocols described in previous publications (*6,16*). The ^{99m}TC-labeled PulmoBind ligand was prepared as described above and the 3 fractions containing the most radioactivity were pooled and used for the assay. Concentration of this initial mixture was 1.527 µM with a specific activity of 81MBq/mmol. Competitive displacement experiments were achieved by incubating 100µL (0.24mg) of dog lung homogenate for 90 min at room temperature in binding buffer (50 mM Tris, 100 mM NaCl, 4 mM $MgCl_2$, 0.1% (w/v) BSA, pH 7.4) with various concentrations (10^{-12}M to 10^{-}

^{5}M) of either unlabeled PulmoBind or AM in the presence of 1nM ^{99m}Tc-labeled PulmoBind. For saturation binding experiments, dog lung homogenates were incubated as described for competitive displacements with increasing concentrations (0.01 nM to 5 nM) of ^{99m}Tc-labeled PulmoBind in the absence (total binding) or presence of 1μM of unlabeled ligand. Incubations were stopped by rapid filtration through glass fiber filter papers pre-soaked in 0.3% polyethyleimine using a Millipore 1225 sampling vacuum manifold (Milford, MA, USA) and after 3 washings, papers were counted on a gamma counter (LKB Wallac 1272 Automatic gamma counter, Gaithersburg, MD, USA).

Hemodynamic Evaluation

Mongrel dogs (male and female) were used to study cardiovascular effects induced by cumulative i.v. injections of human AM(1-52), the agonist hAM(13-52), the antagonist hAM(22-52) and PulmoBind. Heart rate of anesthetized and ventilated animals was monitored with cutaneous electrocardiographic leads and a catheter installed in the right femoral artery was used to monitor blood pressure. Pulmonary artery pressure was evaluated using a Swan-Ganz catheter. Briefly, the catheter was introduced through the jugular vein. From this entry site, it was threaded by fluoroscopy through the right atrium of the heart, the right ventricle, and subsequently into the pulmonary artery until a wedge pressure tracing was noticed. Then, Swan-Ganz catheter balloon was deflated; deflation was confirmed by reappearance of pulmonary artery pressure contours.

Dosimetry Evaluation

The PulmoBind tracer was injected to 7 dogs to estimate the mean biodistribution using whole-body scintigraphic images. Before peptide injection, a whole-body transmission scan was performed on the gamma-camera using a ^{57}Cobalt flood source. The injection syringe was measured prior to injection under the camera. Then, immediately after intravenous injection, dynamic acquisitions were recorded for a 30-min period and static whole body scans were performed at 35, 60 and 120 min after at a scan speed of 10 cm/min. The empty syringe was measured again to determine residual activity.

The biodistribution into organs with significant uptake was evaluated using MATLAB version 7.01 image analysis tools software. Dynamic and whole-body images were first corrected for radioactive decay. Regions of interest were drawn on each organ in anterior and posterior views and on the transmission map. Geometric means of each organ activity were performed and then corrected for average attenuation over the organ. Using syringe images data, results were converted to percentage of the total radioactivity injected.

These animal studies in dogs were performed to get a first approximation of the expected radiation dose absorbed in human subjects. Despite differences between animal and human pharmacokinetic behaviours, an extrapolation process was used to estimate human dosimetry from the calculated dog biodistribution. To

compensate the physiological time difference between species, allometric scaling was applied to the biodistribution curves assuming human physiological time to be 1.19 time slower than the canine one (fourth root of the mass ratio) (17). Individual organs and whole-body-time-activity curves were fitted using the OLINDA software v.1.0 (18). Target organ absorbed radiations were calculated for a 73.7kg standard man and a 56.9kg standard woman models using the same software.

Lung perfusion in pulmonary arterial hypertension

Male Sprague Dawley rats weighting between 200-225 g received a 0.5 mL intraperitoneal injection of either 0.9% saline (n=4) or 60 mg/kg monocrotaline (MCT, n=4). Five weeks later, rats were anesthetized for hemodynamic measurements and nuclear medicine experiments with PulmoBind as previously described (4).

Statistics

Statistical analyses were assessed using the Prism 4.0 software (GraphPad, San Diego, CA, USA) with an unpaired Student t-test or a One Way Anova as indicated in the figure legends.

RESULTS

Synthesis

AM analogs were designed in a simple and straight forward manner based on our previous results using AM as a ^{99m}Tc-labeled imaging agent and known structure-activity relationships. In fact, linear AM had been directly labeled through its free cysteine residues and purified with a SepPak cartridge to obtain a final product of high radiochemical purity (≥95%) (*5*). However, the initial yield of ^{99m}Tc-labeled AM, i.e. before the purification step, was only about 65% (Figure 1). Therefore, we added a chelating moiety to trap the radioisotope. A simple tetrapeptide having ^{99m}Tc chelating properties, Gly-Gly-D-Ala-Gly (*18*) was used. Thus, compound 1 was created by complexing the antagonist AM(22-52) to this tetrapeptide ^{99m}Tc-chelating moiety through a molecular linker, the heterobifunctional polyethylene glycol derivative Fmoc-d(PEG)4-COOH. Two cysteine residues were introduced in the AM analog construction to generate the cyclic compound 2. Finally, compound 3 was designed with Cys(Acm) residues, which cannot form a disulfide bridge since their sulfhydryl moieties are blocked by an Acm group, to verify the impact of cyclization on lung uptake and the influence of cysteine residues in the labelling process.

All peptide syntheses yielded only one major product that was isolated by RP-HPLC and confirmed to be the desired AM analog by Maldi-Tof mass spectrometry analysis. Formation of the disulfide bond was monitored by analytical RP-HPLC, the

cyclized peptide having a shorter retention time than its linear counterpart (results not shown).

^{99m}Tc-Labeling

As expected, the introduction of a chelating moiety greatly improved the ^{99m}Tc-labeling yield of AM analogs as compared to linear AM (Figure 1). In fact, labeling of AM through its free cysteine residues resulted, on average, in 65% of ^{99m}Tc-AM whereas the labeling yield was higher than 80% when using the tetrapeptide as the ^{99m}Tc-chelator. Moreover, the labeling yield obtained with compound 1, 2 and 3 was not markedly affected by the nature of the peptide although yields varied slightly with compound 2 having the highest ability to retain ^{99m}Tc (Figure 1).

***In vivo* Biodistribution and Lung Uptake**

Since very satisfying ^{99m}Tc-labeling yields were obtained with the three AM analogs, their lung uptake ability was evaluated in anesthetized dogs. Purified labeled compound 1, 2 or 3 (radiochemical purity ≥ 95% as evaluated by ITLC analysis) was injected i.v. and a lung dynamic acquisition was performed. All three compounds showed reduced lung uptake as compared to AM (Figure 2). However, compound 2 had a lung first-pass comparable to that observed with AM (around 75% of the injected dose) rapidly followed in the first minute by a 40% uptake plateau maintained for up to 1 h (Figure 2). As for compounds 1 and 3, initial lung uptake was considerably reduced (around 55% of the injected dose) and continuously cleared

from the pulmonary circulation (Figure 2). Interestingly, at 30 min post-injection, compound 2 had a very low heart uptake (3.1 ± 0.3%) even lower than AM (4.9 ± 1.0%) although not significantly different, an important asset to obtain good lung imaging (Figure 3). Moreover, liver uptake for compound 2 was comparable to what was observed with AM. Thus, with a liver uptake of less than 10% (8.2 ± 0.8%) of the injected dose, a lung uptake at least 5 times as high as heart uptake and a lung retention lasting up to 1 h, compound 2 appeared as a good candidate for lung imaging (Figure 4). Further analyses were performed to characterize this compound, renamed PulmoBind.

Binding Assays

To further characterize this new lung imaging agent, binding assays were performed on dog lung homogenates using ^{99m}Tc-PulmoBind as the tracer. Saturation experiments demonstrated that PulmoBind bound to specific binding sites in the dog lung at a density of 2317 ± 320 fmol/mg (Bmax) with an affinity in the nanomolar range (Kd of 2.6 ± 0.8 nM) (Figure 5A, 5B). These values indicated that PulmoBind could occupy more binding sites than AM in the dog lung but with lower affinity. Indeed, a similar set of experiments was performed with AM on the same preparation (*16*) thus allowing the comparison. It had then been evaluated that AM bound specific binding sites at a density of 1222 ± 148 fmol/mg with a Kd of 0.17 ± 0.07 nM.

To verify if PulmoBind had a binding site different than AM in the dog lung, competitive displacement experiments were performed. With either unlabeled AM or PulmoBind, displacement curves were statistically undistinguishable, suggesting that AM and PulmoBind competed for the same binding site in the dog lung (Figure 5C).

Hemodynamic Evaluation

AM is a known vasodilator. When injected i.v. in anesthetized dogs, AM produced a drop in mean arterial blood pressure (MAP) with increasing doses that was accompanied by an elevation in heart rate (HR) (Figure 6A). Similarly, the truncated AM agonist, hAM(13-52), generated decreases in MAP proportional to the increased dose of peptide injected. Noteworthy, the accompanying increase in HR was less pronounced than that observed with AM, although the drop in MAP was similar (Figure 6B). When cumulative doses of hAM(22-52), a specific AM antagonist, were injected, no changes in MAP nor HR were observed even at a dosage equal to 50 times the initial injection (Figure 6C). In a similar manner, cumulative i.v. injections of PulmoBind, which is derived from the latter antagonist, did not produce significant variations of MAP and HR, suggesting that this new lung imaging agent also acts as an antagonist (Figure 6D). Finally, mean pulmonary artery pressure (MPAP) did not vary significantly following injections of hAM(22-52) or PulmoBind, and was within expected values.

Dosimetric Analysis

A dosimetric analysis of PulmoBind is shown in Table 2. This analysis is extrapolated to human using the biodistribution obtained from dogs. The analysis reveals a favourable profile with rapid elimination of the tracer into urine and digestive tract with kidneys receiving the highest radiation dose (0.034mGy/MBq; Table 2). Total effective dose was evaluated under allometric scaling to be 0.0075 and 0.0094 mSv/MBq for a man and woman respectively after 2h (Table 3).

Pulmonary arterial hypertension model

As shown in figure 7, the in vivo biodistribution revealed a markedly reduced lung uptake of PulmoBind from 12 ± 2% ID in controls to 4 ± 1% in PAH, $P<0.001$.

DISCUSSION

Nuclear medicine offers clinicians novel avenues for diagnosis and therapy of various pathological conditions with non-invasive and rapid techniques. In fact, success of nuclear medicine relies on the effectiveness of radiopharmaceutical compounds. These compounds, consisting of a target-specific moiety and a radionuclide, must be well designed and finely tuned to attain the desired results for a particular purpose. Because of their inherent specificity, antibodies are

biomolecules of interest to generate pharmaceutical compounds. However, their poor pharmacokinetics and their tendency to evoke an immunogenic response (20) limit their effectiveness. On the other hand, peptides are also highly specific biomolecules that proved to be useful targeting moieties to generate therapeutic or imaging agents (21,22) with the advantage of being practically devoid of immunogenicity and showing favourable pharmacokinetics (rapid clearance from blood). Moreover, they are quite flexible in terms of chemical modification allowing radiolabelling (23). As such, we have previously shown that the linear AM peptide, once labelled with ^{99m}Tc, was an attractive lung imaging agent for PE diagnosis (*5*). Lung perfusion scintigraphy with ^{99m}Tc-macroaggregates of albumin (^{99m}Tc-MAA) is generally considered as a method of choice in the diagnosis of PE. However, this imaging technique relies on the capture of ^{99m}Tc-MAA in the pulmonary bloodstream causing temporary micro-embolisms in a sufficient amount to generate a good image (24). If the pulmonary circulation is already compromised such as in subjects with severe PH, this procedure could have deleterious effects and some safety issues have been pointed out for patients suffering from pulmonary hypertension or presenting a right-left shunt (24). Thus, a lung imaging agent such as an AM derivative would expand the clinical relevance of lung scintigraphy because of its ability to image all size of vascular beds without any blockade. Moreover, AM binding sites being mostly distributed on the pulmonary microvascular endothelium, a molecular imaging agent based on this peptide could also offer a new diagnostic avenue for PH since this

pathology is associated with microvascular occlusions and endothelial dysfunction not detectable with ^{99m}Tc-MAA (with the exception of chronic thromboembolic PH). Thus, we have demonstrated the relevance of this approach using a monocrotaline-induced PH rat model (*4*). However, AM is a biologically active peptide. As a vasodilator, it could be perceived as beneficial especially if used for PH diagnosis. In fact, AM is recognized as a cardio-renoprotective modulator (25). But AM also stimulates angiogenesis, a less desirable outcome (26). Although nuclear medicine imaging agents are generally utilized at a dose devoid of any biological effect, safety of the clinical procedure is a crucial issue that prompted us to develop a lung imaging agent with antagonist pharmacology.

Many chelators exist to trap ^{99m}Tc, including DTPA (Diethylene Triamine Pentaacetic acid), MAG3 (Mercaptoacetyl Tri-glycine) and HYNIC (6-Hydrazinopyridine-3-carboxylic acid) but the use of a simple tetrapeptide having ^{99m}Tc chelating properties appeared more attractive because it is introduced to the peptide chain during synthesis following the same procedure used for all other amino acids. Incorporation of this peptide chelating moiety greatly improved the labeling yield without any significant difference between the 3 compounds synthesized (Figure 1). A difference appeared when lung uptake was evaluated. As a matter of fact, the presence of a cyclic structure proved to be crucial for efficient lung uptake because just 10 min after injection, about 20% of the linear AM analogs (compounds 1 and 3) remained in the lung whereas more than 40% of AM and the cyclic analog (compound

2) were retained in the organ, with maintenance of this activity even after 30 min (Figure 2). These results are in accordance with structure-activity relationship studies of peptides belonging to the calcitonin family. Circular dichroism analyses of AM demonstrated that the peptide possesses a structure composed of 28% α-helix and 18% β-sheet. Interestingly, the antagonist AM(22-52) shares these structural features (*14*). However, the ring structure composed of 6 residues linked by a disulfide bridge is a common characteristic to all calcitonin peptide family members despite their low sequence homology and it has been shown to be important for proper binding and subsequent signalling (*13,26*). Moreover, amino acid substitution within the ring structure does not seem to alter potently the peptide biological activity (26). Therefore, combining AM(22-52) to a flexible ring structure composed of 2 cysteine residues linked by a PEG spacer to substitute the 6 residues generated a molecule encompassing all important AM structural features to ensure proper receptor binding while avoiding a biological response. In fact, the use of a PEG_4 spacer allowed appropriate spacing without introducing reactive or sensitive chemical groups or increasing too much the hydrophobicity of the molecule. Furthermore, the chelating moiety was added at the N-terminus of the peptide since it was demonstrated that labeling of the peptide at any other position could affect receptor interaction (*16*). Results from our binding study correlate furthermore with AM structure-activity relationships. Indeed, AM was shown to have a Kd of 0.17 ± 0.07 nM on dog lung homogenates (*16*) while PulmoBind (compound 2) has a Kd of 2.6 ± 0.8 nM on the

same preparation (Figure 5). It has to be pointed out that using the same conditions to evaluate binding, AM(22-52) had about 100 times less binding affinity than AM and even linear AM (reduced disulfide bridge) had markedly reduced affinity (*6*). Thus, adding a cyclic structure to AM(22-52) to generate our PulmoBind analog has enhanced binding significantly. Moreover, the number of accessible binding sites appears to be higher for PulmoBind than AM since Bmax values are 2317 ± 320 fmol/mg (Figure 5) and 1222 ± 148 fmol/mg, respectively (*16*). This observation can be related to studies on somatostatin, corticotrophin releasing factor and bombesin demonstrating that radioactive ligand antagonists label more receptor binding sites than corresponding agonists (11,27,28). Therefore, it appears that the slight binding affinity loss of PulmoBind is compensated by a higher number of accessible binding sites that allows a pulmonary circulation imaging similar to that observed with the full AM peptide labelled with ^{99m}Tc.

As previously mentioned, AM disulfide ring structure is implicated in proper receptor interaction and the receptor signalling process. Accordingly, PulmoBind cyclic moiety has enhanced receptor binding but this analog appears to still act as an antagonist like its parent molecule as observed through *in vivo* hemodynamic evaluation (Figure 6). In fact, AM(22-52) did not evoke any changes in MAP, HR or MPAP even at 50 times the imaging dosage and similar observations were obtained with PulmoBind thus suggesting that an AM based imaging agent such as PulmoBind should not show any acute toxicity effects on the pulmonary vascular system during

the course of the examination. In opposition, the truncated AM analog comprising the ring structure, i.e. AM(13-52), elicited a vasodilating response with only 2.5 times the imaging dosage just like AM. Interestingly, the increase in HR was less important with the N-terminal truncated analog, suggesting that this portion of the peptide might be responsible, at least in part, for this specific biological response.

When designing targeted imaging compounds, the goal is to obtain high tissue specificity with a high signal-to-noise ratio, appropriate pharmacodynamics and good pharmacokinetics. Injection of PulmoBind in anesthetized dogs generated a good lung image with low heart and liver uptake, an essential feature for pulmonary vasculature imaging, even 60 min after the injection (Figure 4). The lung kinetic profile of PulmoBind was characterized by an uptake plateau suggesting irreversible binding to its pulmonary receptor. As determined by our in-vivo biodistribution study, PulmoBind was not only retained in pulmonary circulation but also in kidneys (Figure 3). As a matter of fact, labeling of kidneys and bladder were higher than other tissues at later time points with a concomitant decrease in lung, heart and liver uptake indicating that the molecule was eliminated mainly through renal excretion. This clearance route had also been observed with AM labeled with ^{99m}Tc (*5*). Thus, PulmoBind appears to offer good pulmonary circulation imaging properties, without adverse hemodynamic effects and with urinary elimination, qualities making it a very promising compound for clinical use. However, this elimination route is associated with our finding that kidneys are the critical organ in terms of radiation dose.

Moreover, the urinary tract being in close proximity to radiation sensitive tissues such as reproductive organs could be a safety concern but our dosimetry analysis revealed that testes and ovaries were receiving the least radiation among the evaluated organs (Table 2) and even the kidneys were submitted to doses lower than other critical organs identified with clinically used ^{99m}Tc-radiopharmaceuticals (Table 3). Finally, with the proposed injected activity (185-555MBq), the total effective radiation dose (1.7-5.2 mSv for a woman) would be comparable to actual nuclear medicine procedures since doses of 0.2-14 mSv are standardly used in clinical radiographic examinations (*29)*.

Finally, we demonstrated that radiolabeled PulmoBind could detect lung microcirculatory perfusion defect associated with PAH using the MCT model. This model causes progressive obliteration of pulmonary vessels and we have demonstrated that it is associated with a reduced lung expression of the specific heterodimeric component of the AM receptor, RAMP2 (4). There is also previous evidence for the abundant distribution of AM receptors in the pulmonary microcirculation. A study evaluating the distribution of the calcitonin receptor-like receptor (CLR), the other heterodimeric component of the specific AM receptor (CLR-RAMP2), demonstrated intense staining in the lung capillaries (30). Another study demonstrated co-localisation of endothelial cell marker and CLR in pulmonary capillaries and lung endothelial cell expression of CLR and RAMP2 (31).

CONCLUSION

Since nuclear medicine definitely benefits from precise targeting, development of specific radiotherapeutic drugs and medical imaging agents has attracted a lot of interest, with peptides and proteins forming a great part of the starting material. As such, a wide variety of peptides have been used to create new specific radiopharmaceutical compounds but our work supports studies achieved with somatostatin indicating the usefulness of peptide antagonists as nuclear medicine agents (27,32). PulmoBind, an adrenomedullin analog, binds AM receptors found in high density in the pulmonary microvascular endothelium with high affinity without causing any adverse hemodynamic response after systemic injection. Once labeled with ^{99m}Tc, it provides good pulmonary circulation imaging with a nuclear medicine camera that lasts at least for 1h, and the compound is efficiently eliminated through renal excretion. Thus, PulmoBind is a ^{99m}Tc-radiopharmaceutical with the potential to provide new molecular diagnostic modalities for pathologies such as pulmonary hypertension and pulmonary embolism.

ACKNOWLEDGEMENTS

This work was supported by PulmoScience Inc., Canadian Institutes of Health Research, and Montreal Heart Institute Foundation.

REFERENCES

1. Ruppert A, Lees M, Steinle T. Clinical burden of venous thromboembolism. *Curr Med Res Opin.* 2010;26:2465-2473.
2. Badesch DB, Champion HC, Sanchez MA, et al. Diagnosis and assessment of pulmonary arterial hypertension. *J Am Coll Cardiol.* 2009;54(1 Suppl):S55-66.
3. Petersson J, Sanchez-Crespo A, Larsson SA, Mure M. Physiological imaging of the lung: single-photon-emission computed tomography (SPECT). *J Appl Physiol.* 2007;102:468-476.
4. Dupuis J, Harel F, Fu Y, et al. Molecular imaging of monocrotaline-induced pulmonary vascular disease with radiolabeled linear adrenomedullin. *J Nucl Med.* 2009;50:1110-1115.
5. Harel F, Fu Y, Nguyen QT, et al. Use of adrenomedullin derivatives for molecular imaging of pulmonary circulation. *J Nucl Med.* 2008;49:1869-1874.
6. Fu Y, Letourneau M, Nguyen QT, Chatenet D, Dupuis J, Fournier A. Characterization of the adrenomedullin receptor acting as the target of a new radiopharmaceutical biomolecule for lung imaging. *Eur J Pharmacol.* 2009;617:118-123.
7. Dupuis J, Caron A, Ruel N. Biodistribution, plasma kinetics and quantification of single-pass pulmonary clearance of adrenomedullin. *Clin Sci (Lond).* 2005;109:97-102.

8. Edwards WB, Xu B, Akers W, et al. Agonist-antagonist dilemma in molecular imaging: evaluation of a monomolecular multimodal imaging agent for the somatostatin receptor. *Bioconjug Chem.* 2008;19:192-200.

9. Brom M, Oyen WJ, Joosten L, Gotthardt M, Boerman OC. 68Ga-labelled exendin-3, a new agent for the detection of insulinomas with PET. *Eur J Nucl Med Mol Imaging.* 2010;37:1345-1355.

10. Reubi JC, Maecke HR. Peptide-based probes for cancer imaging. *J Nucl Med.* 2008;49:1735-1738.

11. Ginj M, Zhang H, Waser B, et al. Radiolabeled somatostatin receptor antagonists are preferable to agonists for in vivo peptide receptor targeting of tumors. *Proc Natl Acad Sci USA.* 2006;103:16436-16441.

12. Hamid SA, Baxter GF. Adrenomedullin: regulator of systemic and cardiac homeostasis in acute myocardial infarction. *Pharmacol Ther.* 2005;105:95-112.

13. Eguchi S, Hirata Y, Iwasaki H, et al. Structure-activity relationship of adrenomedullin, a novel vasodilatory peptide, in cultured rat vascular smooth muscle cells. *Endocrinology.* 1994;135:2454-2458.

14. Robinson SD, Aitken JF, Bailey RJ, Poyner DR, Hay DL. Novel peptide antagonists of adrenomedullin and calcitonin gene-related peptide receptors: identification, pharmacological characterization, and interactions with

position 74 in receptor activity-modifying protein 1/3. *J Pharmacol Exp Ther.* 2009;331:513-521.

15. Champion HC, Nussdorfer GG, Kadowitz PJ. Structure-activity relationships of adrenomedullin in the circulation and adrenal gland. *Regul Pept.* 1999;85:1-8.

16. Fu Y, Letourneau M, Chatenet D, Dupuis J, Fournier A. Characterization of iodinated adrenomedullin derivatives suitable for lung nuclear medicine. *Nucl Med Biol.* 2011;38:867-874.

17. Boxenbaum H. Interspecies scaling, allometry, physiological time, and the ground plan of pharmacokinetics. Journal of pharmacokinetics and biopharmaceutics. 1982;10:201-227

18. Stabin MG, Siegel JA. Physical models and dose factors for use in internal dose assessment. *Health phys.* 2003;85:294-310.

19. Vanbilloen HP, De Roo MJ, Verbruggen AM. Complexes of technetium-99m with tetrapeptides containing one alanyl and three glycyl moieties. *Eur J Nucl Med.* 1996;23:40-48.

20. Olafsen T, Wu AM. Antibody vectors for imaging. *Semin Nucl Med.* 2010;40:167-181.

21. Correia JD, Paulo A, Raposinho PD, Santos I. Radiometallated peptides for molecular imaging and targeted therapy. *Dalton Trans.* 2011;40:6144-6167.

22. Tweedle MF. Peptide-targeted diagnostics and radiotherapeutics. *Acc Chem Res.* 2009;42:958-968.

23. Chen K, Conti PS. Target-specific delivery of peptide-based probes for PET imaging. *Adv Drug Deliv Rev.* 2010;62:1005-1022.

24. Zophel K, Bacher-Stier C, Pinkert J, Kropp J. Ventilation/perfusion lung scintigraphy: what is still needed? A review considering technetium-99m-labeled macro-aggregates of albumin. *Ann Nucl Med.* 2009;23:1-16.

25. Bunton DC, Petrie MC, Hillier C, Johnston F, McMurray JJ. The clinical relevance of adrenomedullin: a promising profile? *Pharmacol Ther.* 2004;103:179-201.

26. Kuwasako K, Kitamura K, Nagata S, Hikosaka T, Takei Y, Kato J. Shared and separate functions of the RAMP-based adrenomedullin receptors. *Peptides.* 2011;32:1540-1550.

27. Cescato R, Maina T, Nock B, et al. Bombesin receptor antagonists may be preferable to agonists for tumor targeting. *J Nucl Med.* 2008;49:318-326.

28. Perrin MH, Sutton SW, Cervini LA, Rivier JE, Vale WW. Comparison of an agonist, urocortin, and an antagonist, astressin, as radioligands for characterization of corticotropin-releasing factor receptors. *J Pharmacol Exp Ther.* 1999;288:729-734.

29. Mettler FA, Jr., Huda W, Yoshizumi TT, Mahesh M. Effective doses in radiology and diagnostic nuclear medicine: a catalog. *Radiology.* 2008;248:254-263.

30. Hagner S, Stahl U, Knoblauch B, McGregor GP, Lang RE. Calcitonin receptor-like receptor: Identification and distribution in human peripheral tissues. *Cell Tissue Res*. 2002;310:41-50

31. Hagner S, Haberberger R, Hay DL, Facer P, Reiners K, Voigt K, McGregor GP. Immunohistochemical detection of the calcitonin receptor-like receptor protein in the microvasculature of rat endothelium. *Eur J Pharmacol*. 2003;481:147-151

32. Wild D, Fani M, Behe M, et al. First clinical evidence that imaging with somatostatin receptor antagonists is feasible. *J Nucl Med.* 2011;52:1412-1417.

Figure Legends

Figure 1. ^{99m}Tc-labeling yields of AM and its analogs. Reaction mixtures obtained after the ^{99m}Tc-labeling procedure were submitted to ITLC to determine the relative proportion of radioactive species, i.e. free ^{99m}Tc, colloids and labeled peptide. Results are expressed as mean ± SEM of 4 experiments and significant differences with AM were determine by a OneWay ANOVA (Tukey's post-test) with **P*<0.05, ***P*<0.01 and ****P*<0.001.

Figure 2. *In vivo* lung uptake of ^{99m}Tc-labeled AM and analogs in dogs. Dynamic acquisitions were recorded with a dual-head camera at a scan speed of 10cm/min over a 2h period after the injection of 185 MBq of purified ^{99m}Tc-labeled compound.

Figure 3. *In vivo* biodistribution of ^{99m}Tc-labeled hAM and PulmoBind. 185 MBq of purified ^{99m}Tc-labeled peptides were injected i.v. in dogs and a static evaluation was performed post-injection using a dual-head gamma camera and the MATLAB software to analyze data. Graph represent data recorded for A) lungs, B) heart, C) liver, D) kidneys and E) bladder with *n* = 7 for hAM and *n* = 5 for PulmoBind. Significant differences were determine by unpaired t-test for PulmoBind vs hAM with ***P*<0.01 and **P*<0.05.

Figure 4. Dog imaging obtained with ^{99m}Tc-PulmoBind 60 min after a 185 MBq i.v. injection showing A) anterior and B) posterior views.

Figure 5. Binding characterization of PulmoBind on dog lung homogenates. A) Saturation of specific binding sites evaluated with increasing concentrations of ^{99m}Tc-PulmoBind. B) Scatchard plot derived from the saturation experiment data. C) Competitive displacement of bound ^{99m}Tc-PulmoBind with increasing concentrations of unlabeled PulmoBind or AM. Results are expressed as percentage of specific binding which is obtained by subtracting the non-specific binding (in the presence of 1μM unlabeled ligand) from the total binding (labeled peptide alone).

Figure 6. Hemodynamic evaluation in dogs of A) AM, B) the agonist AM(13-52), C) the antagonist AM(22-52) and D) PulmoBind. Anesthetised and ventilated mongrel dogs were injected i.v. with cumulative doses of each peptide and heart rate (green line), mean arterial pressure (black line) and mean pulmonary artery pressure (red line) were monitered. The initial dose is referred to as the lung scan dose, i.e. the maximal dose anticipated for humans (555 MBq, 18.5μg) for a phase-1 clinical study. Animal dosage equivalence was computed for body surface area to monitor their hemodynamic effects. Each graph depicts a typical trace obtained from 2 to 7 evaluations.

Figure 7. Images obtained 30 min after an i.v. injection of ^{99m}Tc-PulmoBind in A) vehicule treated Sprague-Dawley rat and B) monocrotaline-treated rat (pulmonary arterial hypertension model). C) Static evaluations of the presence of the radiotracer in lungs 30 and 60 min after injection where performed using a dual head gamma camera and the MATLAB software to analyze data from different animals and significant differences were determined by a Student t-test with *$p < 0.05$. Vehicule treated rats are depicted by white bars whereas monocrotaline-treated rats are represented by black bars.

TABLE 1. Human Adrenomedullin and Peptide Analogs Synthesized

Compound	Sequence	Purity	Theoretical Molecular Mass	Observed Molecular Mass
hAM	Tyr-Arg-Gln-Ser-Met-Asn-Asn-Phe-Gln-Gly-Leu-Arg-Ser-Phe-Gly-Cys-Arg-Phe-Gly-Thr-Cys-Thr-Val-Gln-Lys-Leu-Ala-His-Gln-Ile-Tyr-Gln-Phe-Thr-Asp-Lys-Asp-Lys-Asp-Asn-Val-Ala-Pro-Arg-Ser-Lys-Ile-Ser-Pro-Gln-Gly-Tyr	98%	6028.82	6028.18
hAM(13-52)	Ser-Phe-Gly-Cys-Arg-Phe-Gly-Thr-Cys-Thr-Val-Gln-Lys-Leu-Ala-His-Gln-Ile-Tyr-Gln-Phe-Thr-Asp-Lys-Asp-Lys-Asp-Asn-Val-Ala-Pro-Arg-Ser-Lys-Ile-Ser-Pro-Gln-Gly-Tyr	97%	4533.15	4535.46
hAM(22-52)	Thr-Val-Gln-Lys-Leu-Ala-His-Gln-Ile-Tyr-Gln-Phe-Thr-Asp-Lys-Asp-Lys-Asp-Asn-Val-Ala-Pro-Arg-Ser-Lys-Ile-Ser-Pro-Gln-Gly-Tyr	95%	3576.03	3578.58
1	Gly-Gly-D-Ala-Gly-dPEG4-hAM(22-52)	92%	4064.16	4065.55
2 (PulmoBind)	Gly-Gly-D-Ala-Gly-Cys-dPEG4-Cys-hAM(22-52)	97%	4270.82	4271.71
3	Gly-Gly-D-Ala-Gly-Cys(Acm)-dPEG4-Cys(Acm)-hAM(22-52)	96%	4412.82	4410.34

TABLE 2. Absorbed Radiation Dose Estimates for ^{99m}Tc-PulmoBind

Organs	**Radiation Dose (mGy/MBq)**
Lungs	0.005
Liver	0.012
Kidneys	0.034
Spleen	0.006
Bladder	0.010
Testes	0.002
Ovaries	0.005
Total Body	0.003

TABLE 3. Comparative Dosimetry of ^{99m}Tc-Radiopharmaceuticals (*28*)

Radiopharmaceutical	**Administered Activity (MBq)**	**Critical Organ**	**Total Effective Dose (mSv)**	**Effective Dose (mSv/MBq)**
^{99m}Tc-PulmoBind	185-555	Kidney	1.4-4.2 (M)	0.0075 (M)
			1.7-5.2 (F)	0.0094 (F)
^{99m}Tc-MAA	185	Lung	2.0	0.011
^{99m}Tc-DTPA	370	Bladder	1.8	0.0061
^{99m}Tc-DMSA	370	Kidney	3.3	0.0088

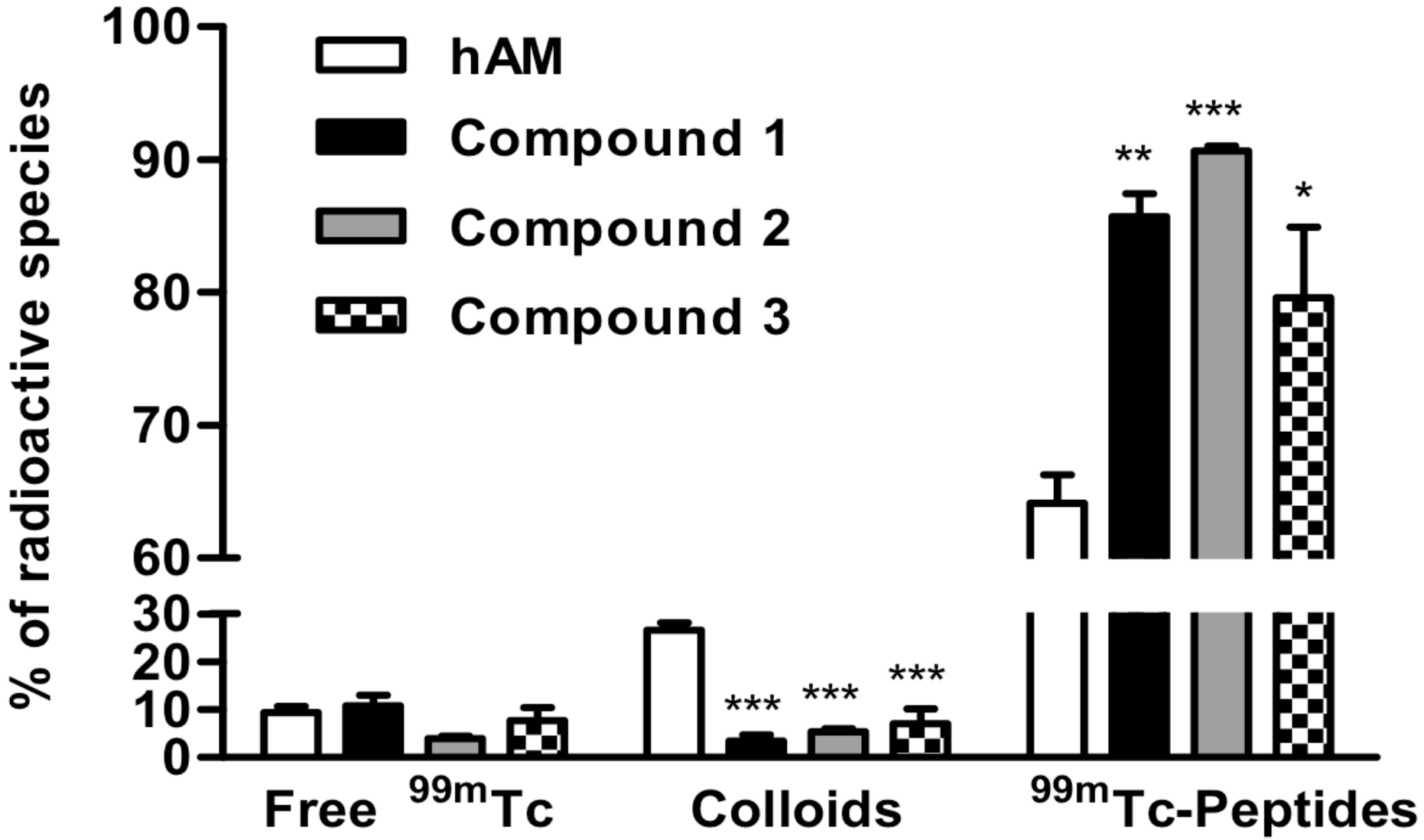
100
90
80
70
60
30
20
10
0
% of radioactive species
hAM
Compound 1
Compound 2
Compound 3
**
***
*
***
***
***
Free 99mTc
Colloids
99mTc-Peptides

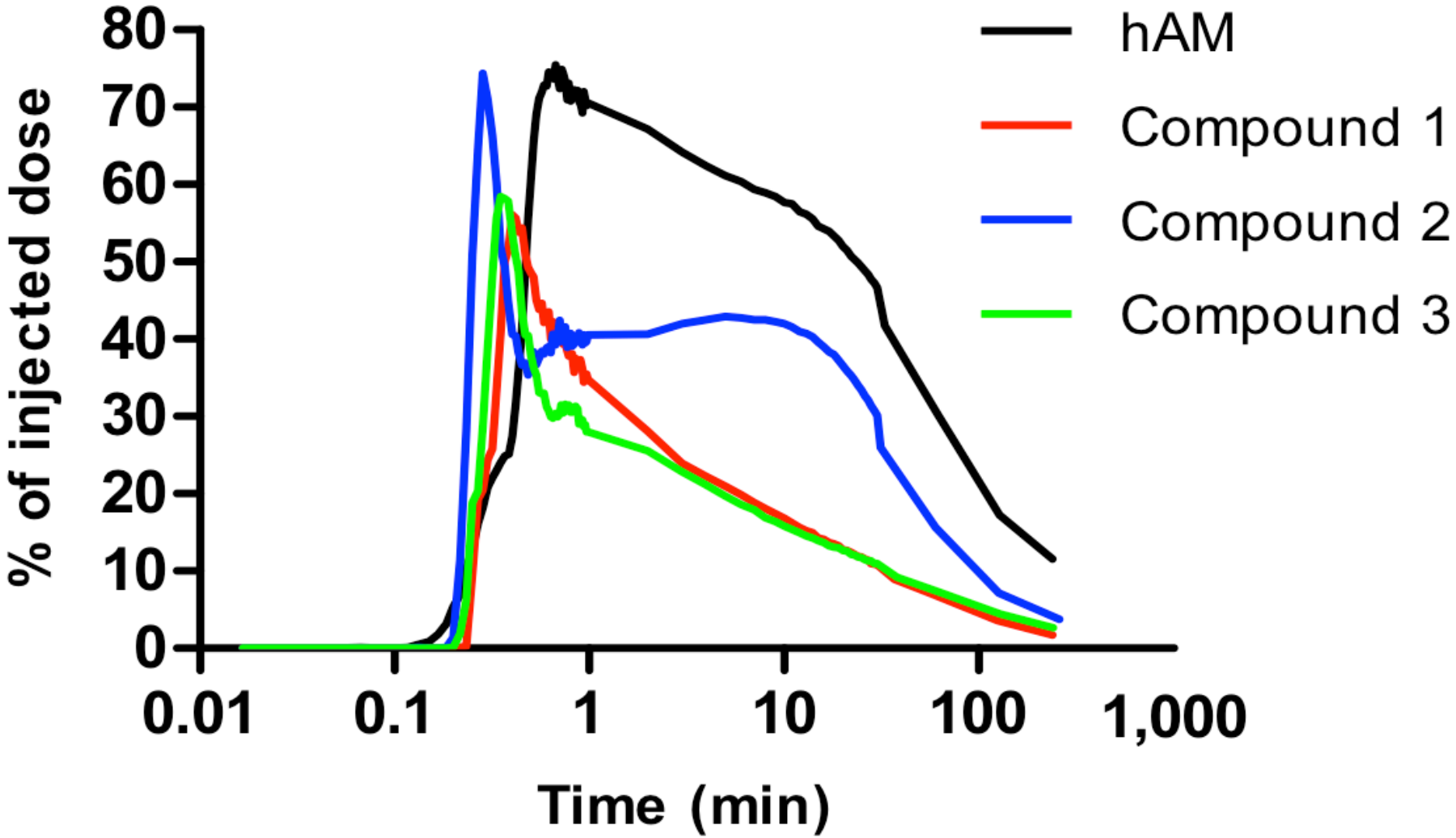
80
70
60
50
40
30
20
10
0
% of injected dose
0.01
0.1
1
10
100
1,000
Time (min)
hAM
Compound 1
Compound 2
Compound 3

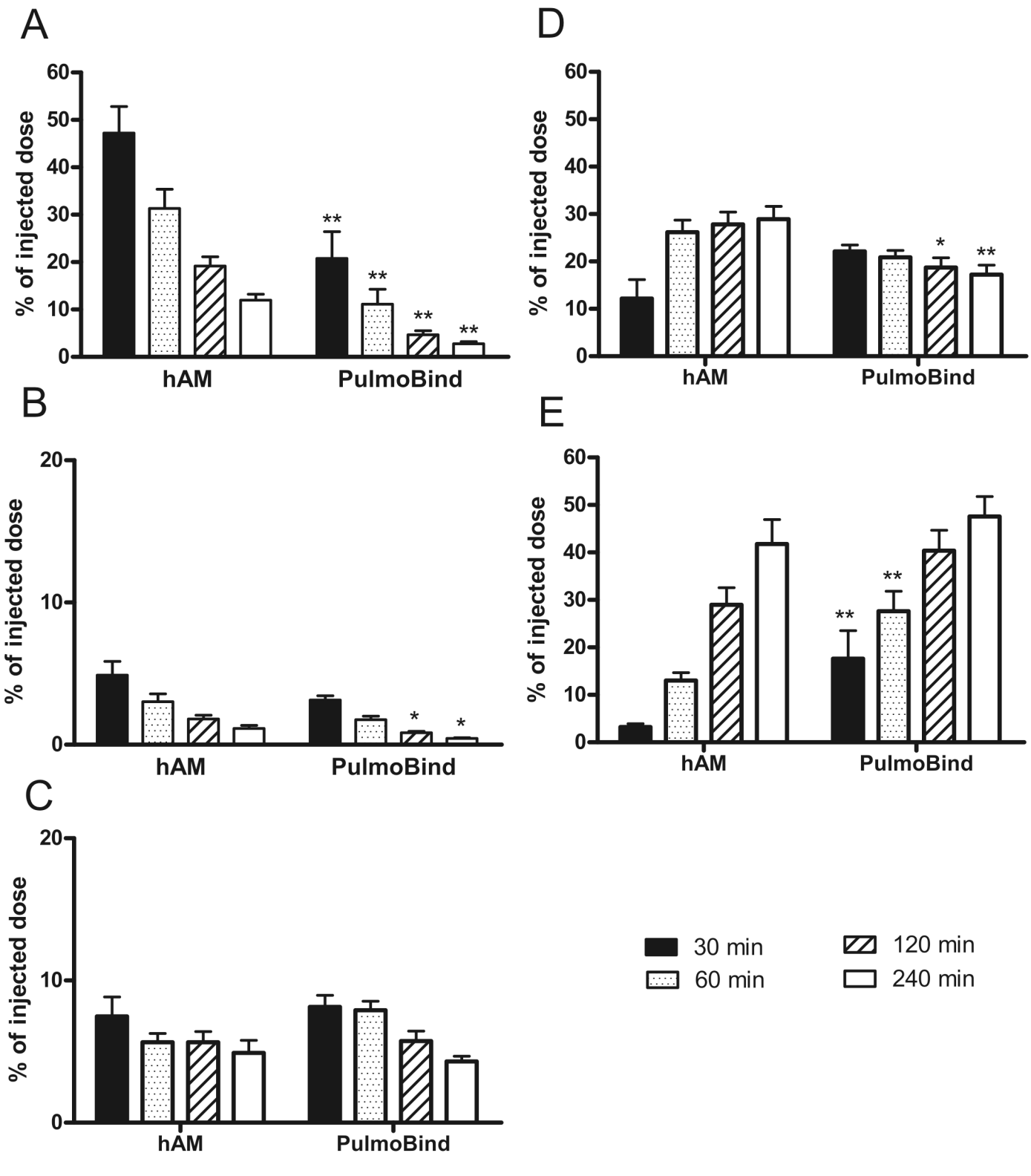
A
B
C
D
E
% of injected dose
hAM
PulmoBind
30 min
60 min
120 min
240 min

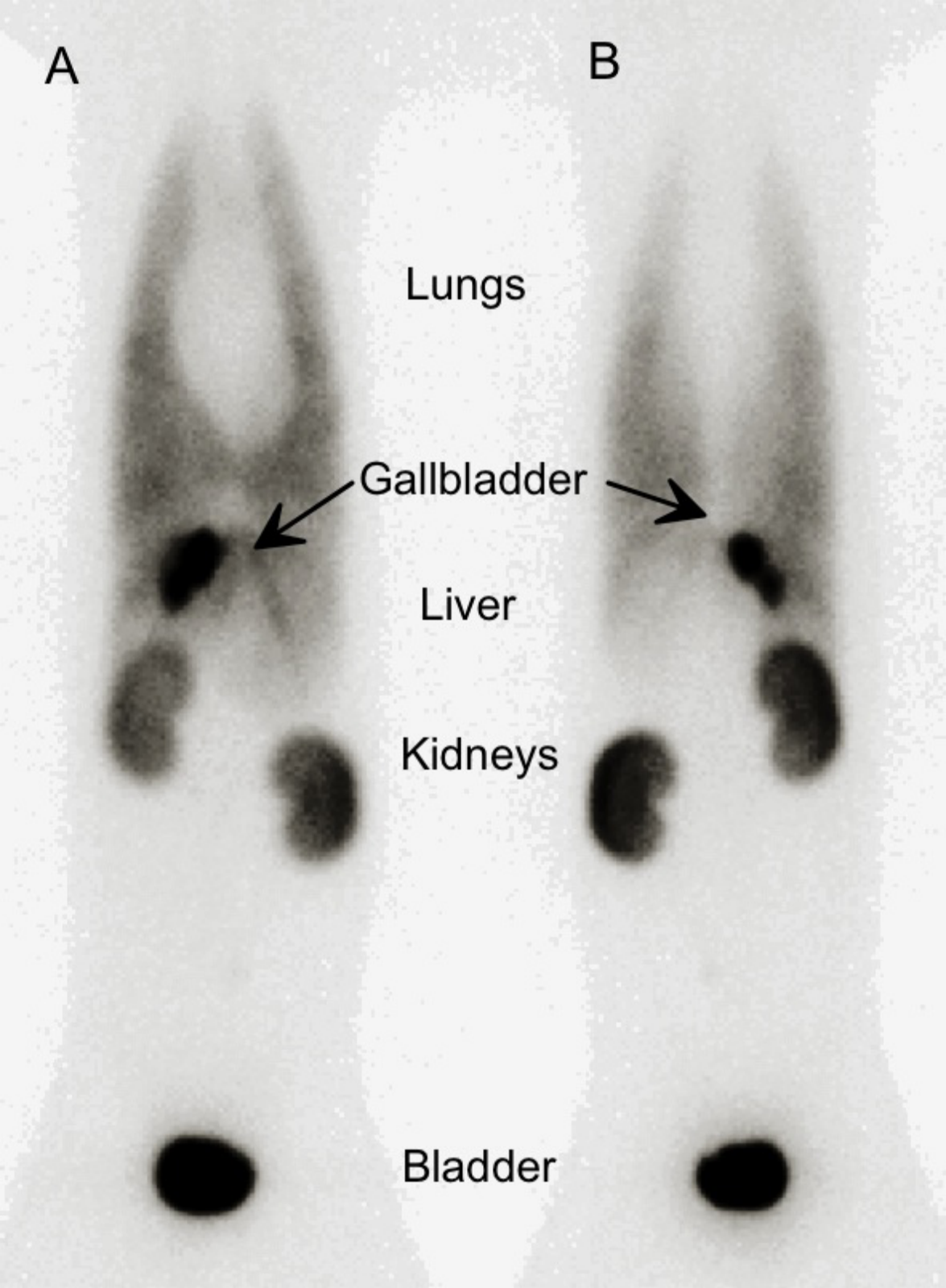
A
B
Lungs
Gallbladder
Liver
Kidneys
Bladder

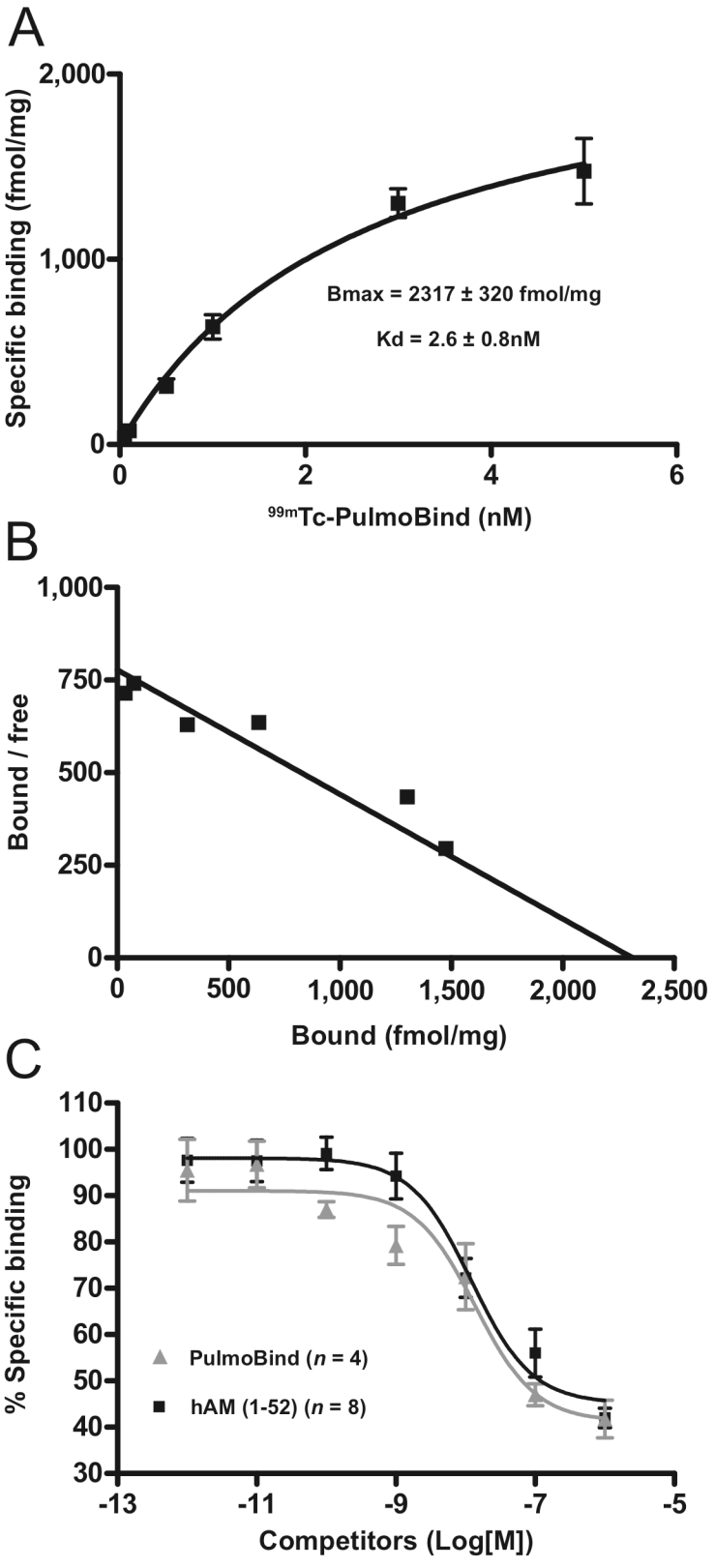
A
Specific binding (fmol/mg)
2,000
1,000
0
Bmax = 2317 ± 320 fmol/mg
Kd = 2.6 ± 0.8nM
0
2
4
6
99mTc-PulmoBind (nM)
B
Bound / free
1,000
750
500
250
0
0
500
1,000
1,500
2,000
2,500
Bound (fmol/mg)
C
% Specific binding
110
100
90
80
70
60
50
40
30
PulmoBind (n = 4)
hAM (1-52) (n = 8)
-13
-11
-9
-7
-5
Competitors (Log[M])

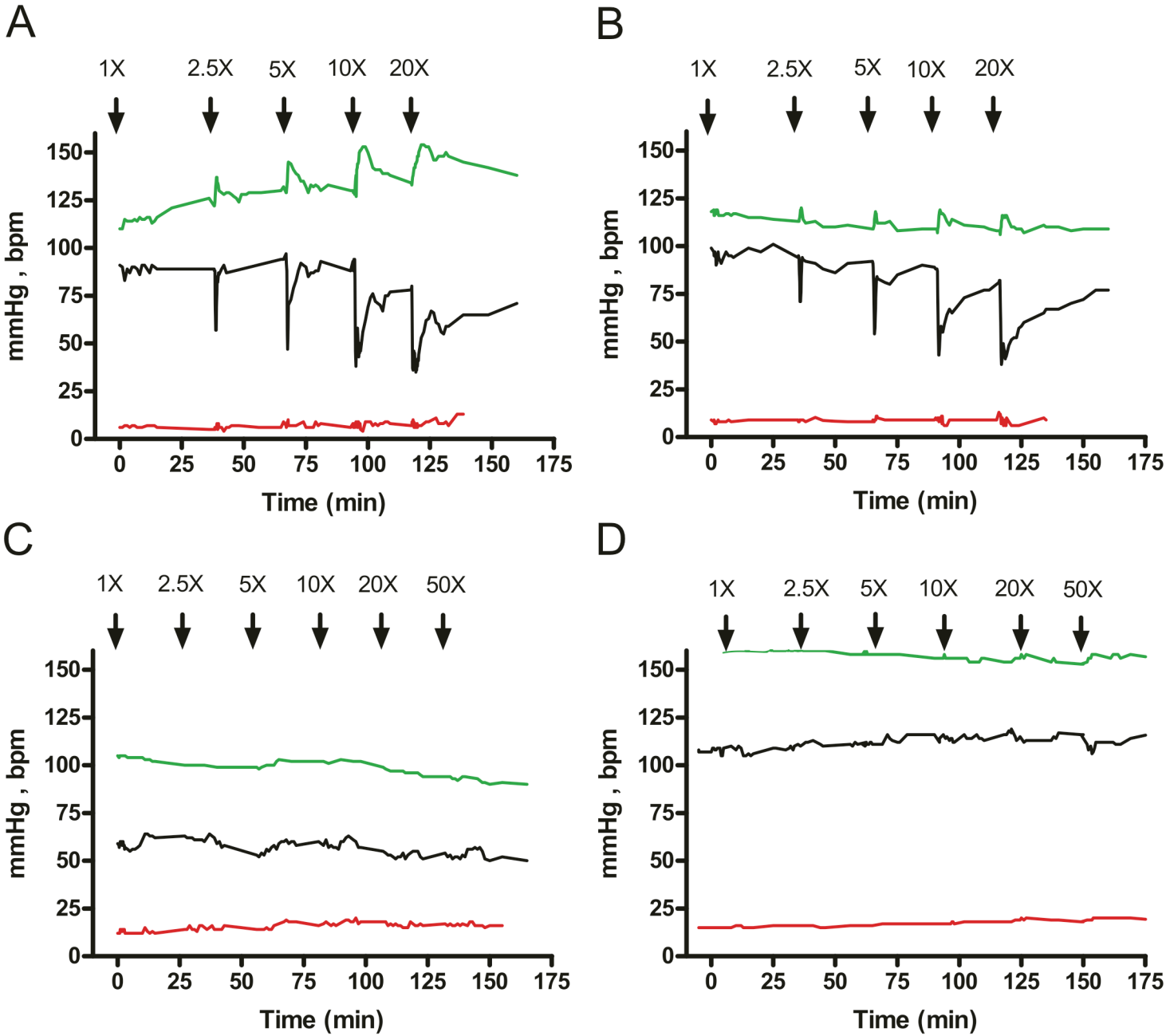
A
1X
2.5X
5X
10X
20X
mmHg , bpm
150
125
100
75
50
25
0
0
25
50
75
100
125
150
175
Time (min)
B
1X
2.5X
5X
10X
20X
mmHg , bpm
Time (min)
C
1X
2.5X
5X
10X
20X
50X
mmHg , bpm
Time (min)
D
1X
2.5X
5X
10X
20X
50X
mmHg , bpm
Time (min)

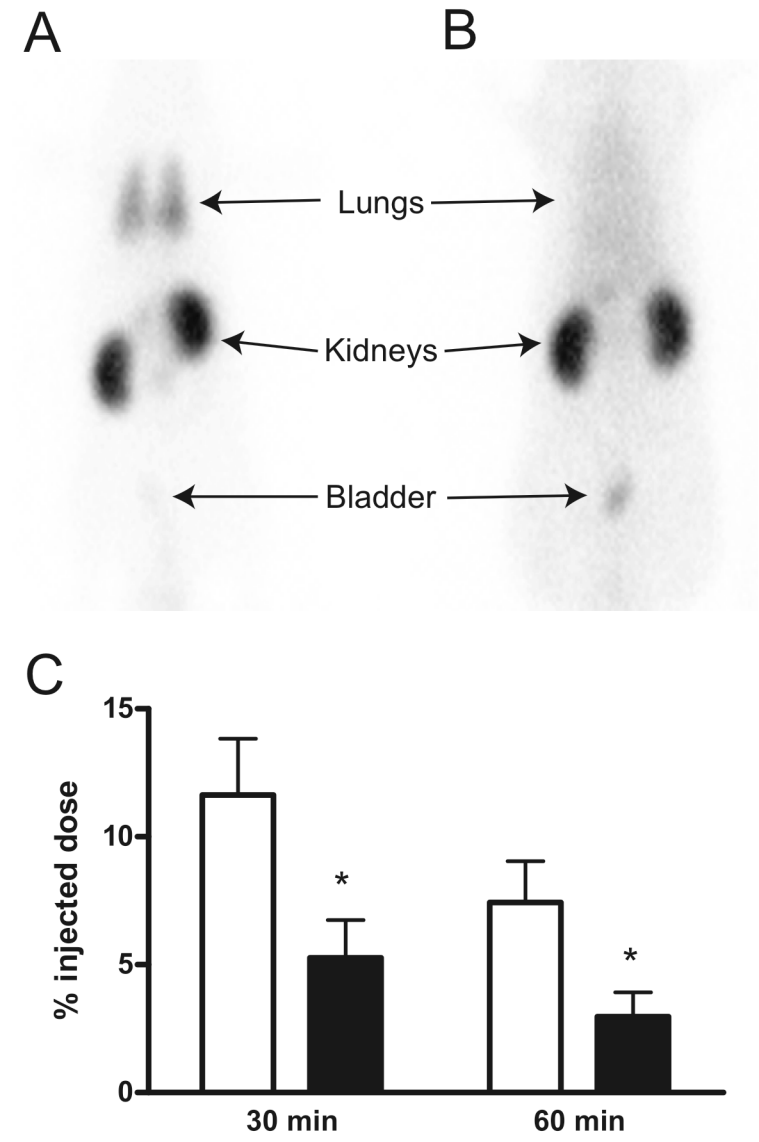
A
B
Lungs
Kidneys
Bladder
C
% injected dose
15
10
5
0
*
*
30 min
60 min